0026-895X/09/7505-1031–1041$20.00
MOLECULAR PHARMACOLOGY
Copyright © 2009 The American Society for Pharmacology and Experimental Therapeutics
Mol Pharmacol 75:1031–1041, 2009

Vol. 75, No. 5
49858/3459128
Printed in U.S.A.

Mitogen-Activated Protein Kinase Pathways Contribute to Hypercontractility and Increased Ca^{2+} Sensitization in Murine Experimental Colitis[S]

Eikichi Ihara, Paul L. Beck, Mona Chappellaz, Josee Wong, Shaun A. Medlicott, and Justin A. MacDonald

Smooth Muscle Research Group, Department of Biochemistry & Molecular Biology (E.I., M.C., J.A.M.), Gastrointestinal Research Group and Department of Medicine (P.L.B., J. W.), and Department of Laboratory Medicine (S.A.M.), University of Calgary, Faculty of Medicine, Calgary, Alberta, Canada

Received June 20, 2008; accepted February 3, 2009

ABSTRACT

Inflammatory bowel disease (IBD) is associated with intestinal smooth muscle dysfunction. Many smooth muscle contractile events are associated with alterations in Ca^{2+}-sensitizing pathways. The aim of the present study was to assess the effect of colitis on Ca^{2+} sensitization and the signaling pathways responsible for contractile dysfunction in murine experimental colitis. Colitis was induced in BALB/c mice by providing 5% dextran sulfate sodium (DSS) in drinking water for 7 days. Contractile responses of colonic circular smooth muscle strips to 118 mM K^+ and carbachol (CCh) were assessed. DSS induced a T_H2 colitis [increased interleukin (IL)-4 and IL-6] with no changes in T_H1 cytokines. Animals exposed to DSS had increased CCh-induced contraction (3.5-fold) and CCh-induced Ca^{2+}-sensitization (2.2-fold) responses in intact and α-toxin permeabilized colonic smooth muscle, respectively. The contributions of extracellular signal-regulated kinase (ERK) and p38 mitogen-activated protein kinase (MAPK) to CCh-induced contractions were significantly increased during colitis. Ca^{2+}-independent contraction induced by microcystin was potentiated (1.5-fold) in mice with colitis. ERK and p38MAPK (but not Rho-associated kinase) contributed to this potentiation. ERK1/2 and p38MAPK expression were increased in the muscularis propria of colonic tissue from both DSS-treated mice and patients with IBD (ulcerative colitis $\gg$ Crohn's disease). Murine T_H2 colitis resulted in colonic smooth muscle hypercontractility with increased Ca^{2+} sensitization. Both ERK and p38MAPK pathways contributed to this contractile dysfunction, and expression of these molecules was altered in patients with IBD.

It has been hypothesized that an imbalance of the T_H1/T_H2 immune response plays a central role in the pathogenesis of inflammatory bowel disease (IBD) (Neurath et al., 2002; Xavier and Podolsky, 2007). The mediators of intestinal inflammation are also known to impair gastrointestinal motility in human disease and animal models, which may be a reflection of altered smooth muscle function. Alterations in gastrointestinal motility with resultant changes in transit contribute to the abdominal pain, intestinal cramping, and diarrhea characteristically associated with IBD. Furthermore, defects in smooth muscle function can lead to the development of toxic megacolon. While it is commonly accepted that smooth muscle contractility is altered in inflamed intestine, there is still considerable disagreement whether intestinal contractility is increased or decreased in IBD. T_H1 and T_H2 immune responses play different roles in dysfunction of smooth muscle contractility. Tumor necrosis factor

This work was supported by the Crohn's and Colitis Foundation of Canada; the Canadian Institutes of Health Research; a Uehara Memorial Foundation Fellowship (Japan); a Canadian Association of Gastroenterology/Canadian Institutes of Health Research/AstraZeneca Fellowship; a Canada Research Chair (Tier II) in Smooth Muscle Pathophysiology; and a Scholarship from the Heart and Stroke Foundation of Canada.

Article, publication date, and citation information can be found at http://molpharm.aspetjournals.org.

doi:10.1124/mol.108.049858.

[S] The online version of this article (available at http://molpharm.aspetjournals.org) contains supplemental material.

ABBREVIATIONS: IBD, inflammatory bowel disease; TNF, tumor necrosis factor; CCh, carbachol; TNBS, 2,4,6-trinitrobenzenesulfonic acid; IL, interleukin; STAT, signal transducer and activator of transcription; LC_{20}, regulatory light chains of myosin II; MLCK, myosin light chain kinase; MLCP, myosin light chain phosphatase; ROK, Rho-associated kinase; ERK, extracellular signal-regulated kinase; MAPK, mitogen-activated protein kinase; DSS, dextran sulfate sodium; PD98059, 2′-amino-3′-methoxyflavone; SB203580, 4-(4-fluorophenyl)-2-(4-methylsulfinylphenyl)-5-(4-pyridyl)1*H*-imidazole; U0126, 1,4-diamino-2,3-dicyano-1,4-bis(methylthio)butadiene; SB202190, 4-(4-fluorophenyl)-2-(4-hydroxyphenyl)-5-(4-pyridyl)1*H*-imidazole; MPO, myeloperoxidase; NES, normal extracellular solution; KES, K^+ extracellular solution; A23187, calcimycin; PAGE, polyacrylamide gel electrophoresis; Y27632, *N*-(4-pyridyl)-4-(1-aminoethyl)cyclohexanecarboxamid; UC, ulcerative colitis; CD, Crohn disease; MYPT1, myosin target subunit of MLCP; pCa, $-\log_{10}$ [Ca^{2+}].

(TNF)-α can attenuate carbachol (CCh)-induced contraction in colonic inflammation induced by 2,4,6-trinitrobenzenesulfonic acid (TNBS) in C57BL/6 mice (Ohama et al., 2007). Alternatively, it was reported that incubation of human cultured smooth muscle cells with T_H2 cytokines, interleukin (IL)-4 or IL-13, enhanced CCh-induced contraction via activation of signal transducer and activator of transcription 6 (STAT6) (Akiho et al., 2005b). Collectively, the T_H1 and T_H2 immune responses are associated with hypocontractility and hypercontractility of inflamed intestinal smooth muscle, respectively.

The contractile properties of smooth muscle are governed by the phosphorylation of regulatory light chains of myosin II (LC_{20}) (Somlyo and Somlyo, 2003; Murthy, 2006), which is driven by the balance between myosin light chain kinase (MLCK) and myosin light chain phosphatase (MLCP) activities. MLCK is activated by Ca^{2+}-calmodulin, thus cytosolic Ca^{2+} concentration ($[Ca^{2+}]_i$) is the primary determinant of smooth muscle contraction. However, MLCP functions independently of Ca^{2+}-calmodulin and is regulated by G protein-coupled signaling pathways. Inhibition of MLCP leads to an increase in both LC_{20} phosphorylation and contractile force development in smooth muscle without any changes in $[Ca^{2+}]_i$. This enhancement of the contractile response to Ca^{2+} is commonly referred to as "calcium sensitization" (Somlyo and Somlyo, 1994). Several protein kinases, including Rho-associated kinase (ROK) (Kimura et al., 1996), protein kinase C (Eto et al., 1997), integrin-linked kinase (Deng et al., 2002; Kiss et al., 2002), and zipper-interacting protein kinase (MacDonald et al., 2001; Borman et al., 2002) are linked to Ca^{2+} sensitization; however, we have recently demonstrated that ERK and p38MAPK are pivotal mediators of Ca^{2+} sensitization in intestinal smooth muscle (Ihara et al., 2007). Alterations in Ca^{2+}-sensitizing pathways are associated with many disorders that involve smooth muscle dysfunction, including hypertension (Seko et al., 2003), vasospasm (Miwa et al., 2005), and colitis (Ohama et al., 2007).

Although the T_H2 immune response was reported to be associated with hypercontractility, its precise underlying mechanisms remain to be determined. In the present study, we examined the protein kinase signaling pathways responsible for increased Ca^{2+} sensitization and contractile dysfunction in murine experimental colitis with an elevation of T_H2 cytokines. We show for the first time that the expression of ERK and p38MAPK was up-regulated and these MAPK pathways played crucial roles in T_H2 cytokine-mediated Ca^{2+} sensitization and hypercontractility observed with inflamed colonic circular smooth muscle from dextran sulfate sodium (DSS)-treated BALB/c mice.

Materials and Methods

Materials. All chemicals were reagent grade unless otherwise indicated. PD98059, SB203580, U0126, SB202190, and β-escin were obtained from Sigma (St. Louis, MO). α-toxin was purchased from List Laboratories, Inc. (Campbell, CA). DSS (mol. wt., 36,000~50,000) was from MP Biomedical (Solon, OH). A23187 was from Calbiochem (San Diego, CA). Microcystin LR was obtained from Alexis Biochemical (San Diego, CA). ERK and p38MAPK Immunoprecipitation Kinase Assay Kits as well as anti-MAP-kinase 1/2 (which recognizes both ERK1 and ERK2 isoforms), anti-phospho MAP kinase (which recognizes the dual-phosphorylation of ERK1 and ERK2 at Thr-200 and Tyr-202), anti-p38MAPK (which recognizes various SAPK2 isoforms), and anti-phospho p38MAPK (which recognizes dual-phosphorylation of SAPK2 isozymes at Thr-180 and Tyr-182) were from Cell Signaling Technology Inc. (Denvers, MA).

Induction and Assessment of Colitis. All animal experimentation was approved by the University of Calgary Animal Care and Use Committee. Colonic inflammation was induced in female BALB/c mice (19–20 g) by administering 5% (w/v) DSS in the drinking water for 7 days, after which time the animals were sacrificed. Myeloperoxidase (MPO) activity was measured as an index of inflammation in samples of the proximal colon as described previously (Beck et al., 2004).

Measurement of Cytokines Released in Colon. Cytokine levels in the colon from normal and DSS-treated mice were measured with the custom Mouse Cytokine Array I (RayBiotech Inc., Norcross, GA). Samples of distal colon, located adjacent to sections used for smooth muscle force measurements, were removed and flash-frozen in liquid N_2. Tissue samples were homogenized 1:20 (w/v) in Cell Lysis Buffer (RayBiotech, Inc.) with Complete protease inhibitor cocktail (Roche, Indianapolis, IN). The homogenate was centrifuged at 14,000 rpm for 5 min at 4°C. Samples of soluble protein were delivered to RayBiotech for detection of cytokines and chemokines. Array results were quantified by densitometry, and the relative expression of indicated cytokines was calculated as a % of the positive control intensity.

Force Measurement of Colonic Circular Smooth Muscle. Normal and DSS-treated mice were sacrificed, and the distal colon was removed. Colonic circular smooth muscle sheets were dissected and cut into strips (250 μm $\times$ 2 mm). For force measurements, muscle strips were tied with silk monofilaments to the tips of two fine wires, one of which was connected to a force transducer (AE801; SensoNor, Horten, Norway). Muscle strips were stretched in the circular axis until the resting force reached to 0.1 mN. Then, the strips were equilibrated for 30 min in normal extracellular solution (NES). Contraction in response to a 118 mM K^+ extracellular solution (KES) was used to assess muscle quality. For intact smooth muscle experiments, force levels observed with NES and KES were designated as 0 and 100%, respectively. In some experiments, we measured the absolute force, which was normalized to the cross-sectional area of the smooth muscle strip. Permeabilized smooth muscle experiments were performed as described previously (Ihara et al., 2007). In brief, muscle strips were incubated either with 50 μM β-escin for 40 min or with 10 μg/ml α-toxin for 60 min in G1 solution with 10 μM A23187 added for the final 10 min to deplete intracellular Ca^{2+} stores. The force levels obtained with relaxing solution (pCa 9 or G10) and pCa 4.5 were designated as 0 and 100%, respectively. All contractile measurements were carried out at room temperature (23°C) with a computerized data acquisition system (PowerLab/8SP data recording unit and Chart software; ADInstruments, Colorado Springs, CO).

Measurement of LC_{20} Phosphorylation. The phosphorylation status of LC_{20} was examined by Phos-Tag SDS-PAGE (Kinoshita et al., 2006a; Takeya et al., 2008). Contractile responses of smooth muscle strips were halted by immersion in a dry-ice/acetone solution containing 10% (w/v) trichloroacetic acid and 10 mM DTT. The muscle strips were washed with an acetone solution containing 10 mM DTT and lyophilized overnight. Muscle protein were extracted in a buffer containing 1% SDS, 30 mM Tris, pH 6.8, 12.5% (v/v) glycerol, and (p-amidinophenyl)methanesulfonyl fluoride with a glass-glass, hand homogenizer. Phos-Tag ligand (final concentration, 30 μM) and $MnCl_2$ (final concentration, 60 μM) were added to the separating-gel (10% polyacrylamide) before polymerization. After electrophoresis, gels were soaked in buffer containing 25 mM Tris, 192 mM glycine, and 2 mM EDTA and were then transferred to polyvinylidene difluoride membranes. Western blotting was carried out with a polyclonal antibody that detects both phosphorylated and unphosphorylated LC_{20}. The stoichiometry of LC_{20} phosphorylation was calculated from the following equation: moles of P_i per moles of

$LC_{20} = (y + 2z)/(x + y + z)$, where x, y, and z are the signal intensities of un-, mono-, and diphosphorylated LC_{20} bands, respectively.

Hematoxylin and Eosin Staining and Immunohistochemistry of Colonic Sections. Segments of mouse colon were fixed, embedded in paraffin and stained with hematoxylin and eosin in a standard fashion (Beck et al., 2004). Paraffin-embedded sections were stained for ERK, phospho-ERK, p38MAPK, and phospho-p38MAPK. Slides were treated to allow for antigen exposure, incubated for 1 h at room temperature in a blocking solution of 5% goat serum in PBST (135 mM NaCl, 1.3 mM KCl, 3.2 mM Na_2HPO_4, 0.5 mM KH_2PO_4, 0.05% Tween 20, and pH 7.4) and then rinsed and incubated with primary antibody (1:100 dilution of ERK and phos-

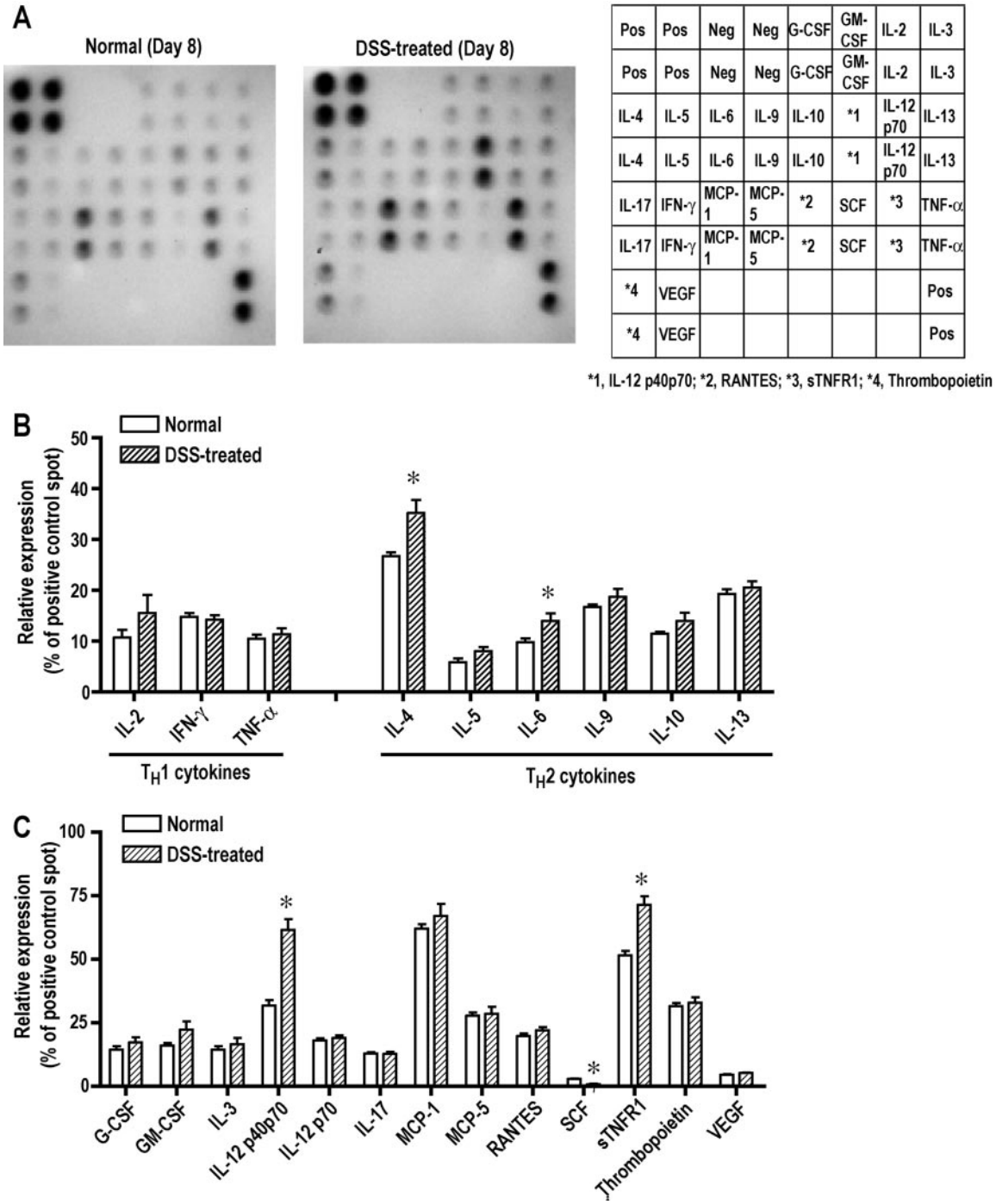

Fig. 1. Cytokine profiles from colon of normal and DSS-treated mice. A, representative images of Raybiotech mouse cytokine antibody arrays. Pos, positive control; Neg, negative control; G-CSF, granulocyte-colony-stimulating factor; GM-CSF, granulocyte-macrophage colony-stimulating factor; IL, interleukin; IFN, interferon; MCP, monocyte chemoattractant protein; RANTES, regulated on activation, normal T-cell expressed and secreted; SCF, stem cell factor; sTNFR1, soluble tumor necrosis factor receptor I; TNF, tumor necrosis factor; VEGF, vascular endothelial growth factor. B, expression levels of T_H1 and T_H2 cytokines released in the colon from normal and DSS-treated mice. The cumulative results were obtained with 6 independent experiments both for normal and DSS-treated mice. The relative expression levels of cytokines were calculated as a % of the positive control intensity. C, expression levels of other cytokines in the mice colonic tissues examined by RayBiotech antibody arrays. The cumulative results were obtained with 6 independent experiments both for normal and DSS-treated mice. The relative expression levels of cytokines were calculated as a % of the positive control intensity.

pho-ERK and 1:50 dilution of p38MAPK and phopho-p38MAPK. Slides were washed with PBST before incubation with biotinylated donkey anti-rabbit polyclonal antibody (1:500 dilution). Slides were washed with PBST, incubated with streptavidin-HRP (1:100 dilution), and then developed with 3-3′-diaminobenzidine solution.

Western Blot Analysis of ERK and p38MAPK. The transverse colon was removed both from normal and DSS-treated mice. Smooth muscle sheets were dissected and flash-frozen in liquid N_2 before homogenization in 20 volumes of sample buffer [1% SDS, 30 mM Tris, pH 6.8, 12.5% (v/v) glycerol, and (p-amidinophenyl)methanesulfonyl fluoride]. Homogenates were resolved on 10% SDS-PAGE gels and then transferred to polyvinylidene difluoride membrane. The blots were blocked with 5% (w/v) nonfat dry milk and then incubated with primary antibody (1:1000 dilution of total-ERK, total-p38MAPK, and β-actin) in 1% (w/v) nonfat dry milk in Tris-buffered saline/Tween 20. The blots were washed and then incubated for 1 h with horseradish peroxidase-conjugated secondary antibody (1:10,000 dilution for total-ERK and total-p38MAPK, and 1:2500 dilution for β-actin) in 1% (w/v) nonfat dry milk in Tris-buffered saline/Tween 20. Blots were developed with enhanced chemiluminescence reagent (GE Healthcare, Chalfont St. Giles, Buckinghamshire, UK). The bands were quantified by densitometry, and the abundance ratio of total-ERK and total-p38MAPK to β-actin was calculated.

Immunohistochemistry of Human Colonic Sections. Human colonic surgical resection tissue was obtained from patients through the University of Calgary CCFC (Crohn's and Colitis Foundation of Canada) Tissue Bank after approval by the University of Calgary Research Ethics Board. Non-IBD (normal tissue from patients undergoing colon cancer resection) and active IBD (CD or UC) tissue samples were obtained from patients under care at Foothills Hospital (Calgary, AB, Canada). Immunohistochemistry of ERK and p38MAPK was performed in a manner similar to that described for mouse colonic sections under *Hematoxylin and Eosin Staining and Immunohistochemistry of Colonic Sections*.

Data Analysis. All data are expressed as the mean ± S.E.M. The Student's t test was used to determine statistical significance with $P < 0.05$ considered to be significant.

Results

Characterization of DSS-Induced Colitis in BALB/c Mice. DSS administration resulted in severe colitis associ-

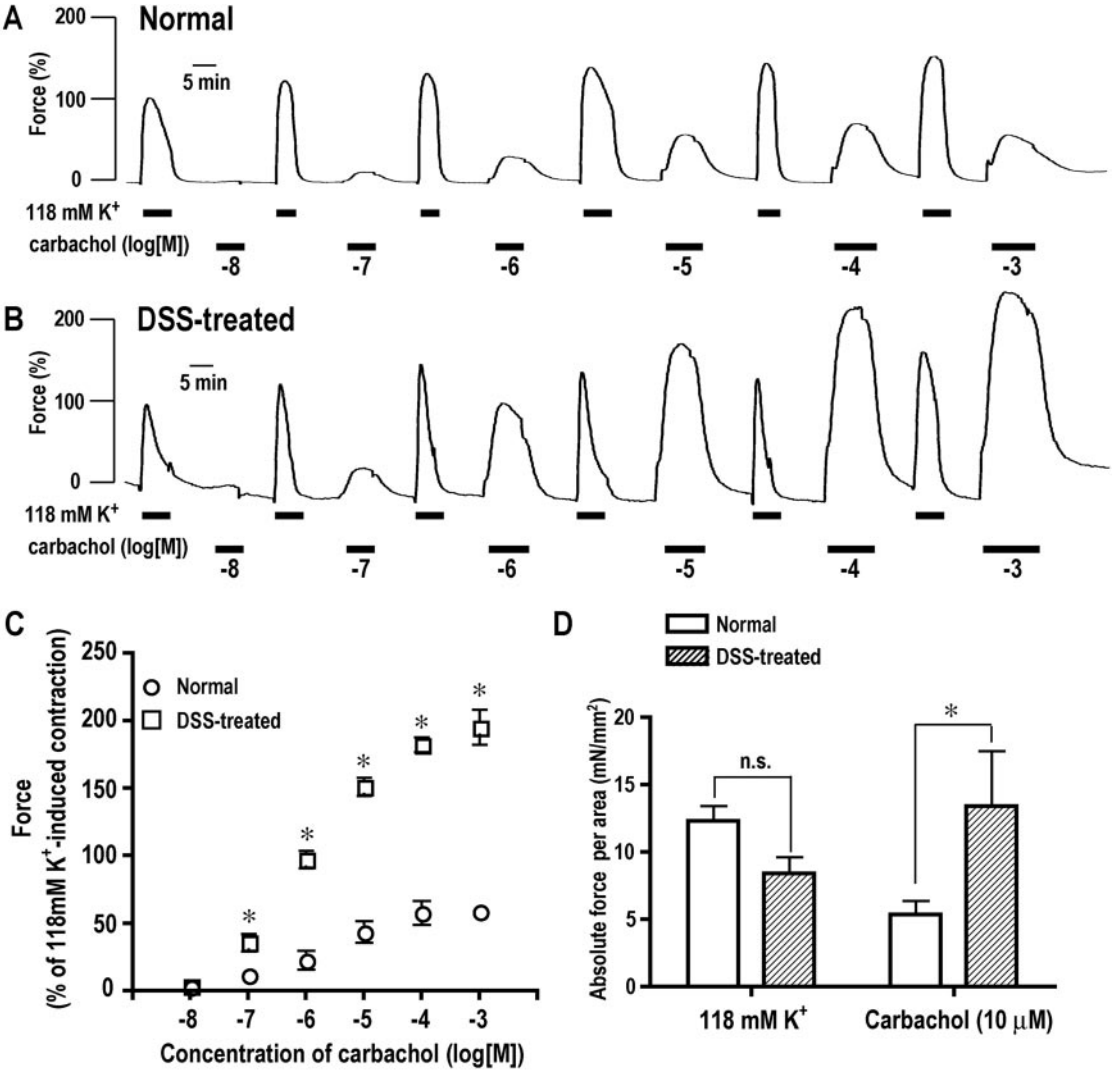

Fig. 2. Contractile responses to 118 mM K^+ and carbachol observed in colonic circular smooth muscle isolated from normal and DSS-treated mice. A and B, concentration-dependent responses to carbachol (10 nM–1 mM) in normal (A) and DSS-treated mice (B) were determined. C, cumulative results are representative of 4 independent experiments. The peak force was measured, and data are expressed as % of 118 mM K^+-induced contraction. D, contractile response to 118 mM K^+ and carbachol (10 μM) in colonic circular smooth muscle isolated from normal and DSS-treated mice are expressed as absolute force development, which was normalized by cross-sectional area of the samples. The cumulative results are representative of 4 independent experiments. Error bars indicate S.E.M. *, significantly different (Student's t test, $P < 0.05$); n.s., not significantly different.

ated with diarrhea, rectal bleeding, and weight loss within 7 days of DSS exposure (Supplemental Fig. 1). MPO is found in the intracellular granules of neutrophils, and MPO activity is used as a marker for tissue neutrophil content and as an index of inflammation (Beck et al., 2004). Upon sacrifice, mice exposed to DSS had significantly ($P = 0.005$) higher levels of colonic MPO activity (2.7 ± 0.3 U/mg protein, $n = 6$) than non-DSS exposed animals (0.36 ± 0.08 U/mg protein, $n = 6$).

Protein cytokine arrays revealed significantly increased expression of the T_H2 cytokines: IL-4 (35.3 ± 2.6%, $n = 6$, $P = 0.030$) and IL-6 (14.1 ± 1.5%, $n = 6$, $P = 0.018$) compared with non-DSS exposed animals (IL-4, 26.8 ± 0.76%, $n = 6$; IL-6, 8.50 ± 0.41%, $n = 6$). Furthermore, there was no difference in the expression of T_H1 cytokines between normal and DSS-treated mice (Fig. 1, A and B). The expression of IL-12 p40p70, but not IL-12 p70, was significantly higher in DSS-treated mice (Fig. 1, A and C). Because the IL-12 p40 subunit is shared with IL-23, these findings suggest that expression of IL-23 is increased in DSS colitis in our BALB/c murine model. In addition, expression of soluble tumor necrosis factor receptor I, which binds to TNFα and is capable of inhibiting TNFα-induced activities by acting as a decoy receptor, was also significantly increased during DSS colitis (Fig. 1, A and C). These data confirm that DSS induces a predominantly T_H2 type of colitis in BALB/c mice.

Contractile Responses to Carbachol in Intact Colonic Circular Smooth Muscle Strips Were Potentiated with DSS-Induced Colitis. The muscarinic receptor agonist CCh generated contractile force in a concentration-dependent manner in colonic circular smooth muscle strips isolated from normal mice (Fig. 2, A and C). It is noteworthy that CCh-induced contractions were much greater in the DSS-treated mice than in normal mice. The force level during 10^{-5} M CCh-induced contraction (151.2 ± 6.9%, $n = 4$) in inflamed colonic circular smooth muscle strips was significantly higher than that observed (43.7 ± 8.0%, $n = 4$) in normal colonic circular smooth muscle strips (Fig. 2, B and C). The absolute force obtained during 10^{-5} M CCh-induced contraction (13.3 ± 4.1 mN/mm^2, $n = 4$) of inflamed colonic circular smooth muscle strips was also significantly higher than that calculated (5.2 ± 1.0%, $n = 4$) for normal colonic circular smooth muscle strips (Fig. 2D). However, there was no significant difference in KES-induced contractile force development between acute inflamed and normal colonic circular smooth muscle strips after DSS exposure (Fig. 2D).

DSS-Induced Colitis Is Associated with Increased Ca^{2+} Sensitization in Circular Smooth Muscle. We examined whether Ca^{2+} sensitization was altered with DSS-induced colitis. Experimentally induced Ca^{2+} sensitization can be elicited in α-toxin permeabilized smooth muscle by application of carbachol, after the induction of submaximal contraction with calcium. The additional force development is defined herein as CCh-induced Ca^{2+} sensitization. The contractile responses to a submaximal calcium solution (pCa 6.3; 500 μM) were similar in α-toxin permeabilized smooth muscle from normal and DSS-treated mice (Fig. 3, A and B). The contractile force gradually developed and then reached a sustained level (around 35% of maximal contraction). It is noteworthy that the extent of CCh-induced Ca^{2+} sensitization (21.1 ± 1.4%, $n = 4$) was significantly higher in DSS-treated mice than that found (9.5 ± 0.85%, $n = 4$) in control mice (Fig. 3C). These findings indicate that agonist-induced pathways of Ca^{2+} sensitization were increased in inflamed colonic circular smooth muscle.

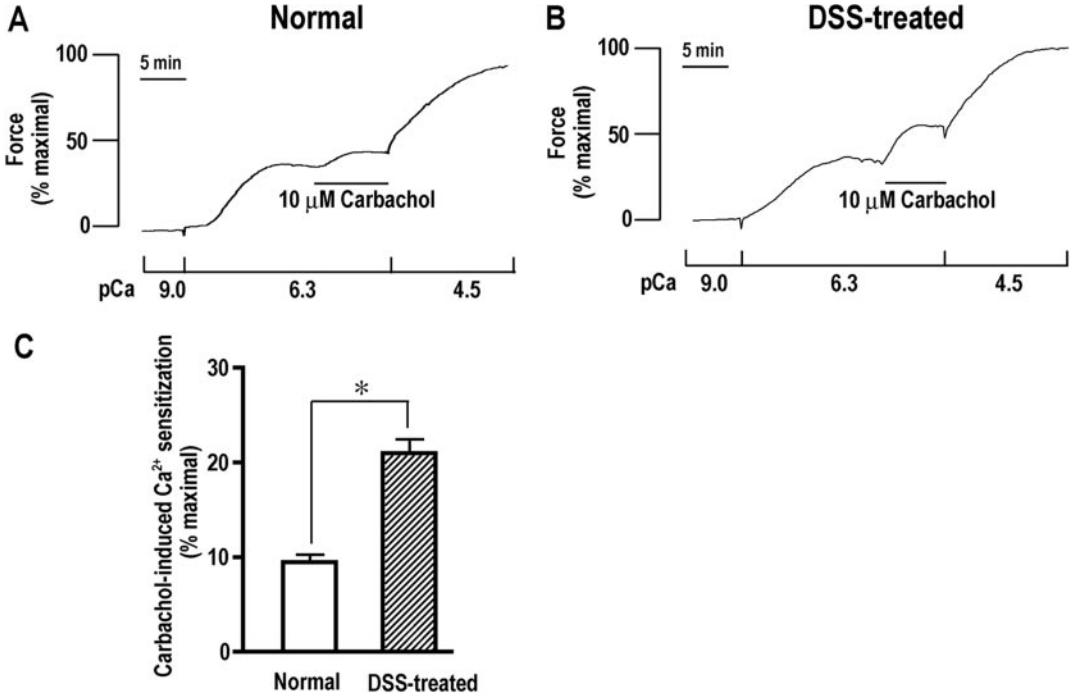

Fig. 3. Carbachol-induced Ca^{2+} sensitization in α-toxin permeabilized colonic circular smooth muscle strips from normal and DSS-treated mice. A and B, representative recordings of carbachol-induced Ca^{2+} sensitization in normal (A) and DSS-treated mice (B) are shown. Carbachol (10 μM) was applied to the strips during the plateau of pCa 6.3 contraction. Forces observed at pCa 9 and pCa 4.5 were designated as 0% and 100%, respectively. C, the cumulative results are representative of 5 independent experiments for carbachol-induced Ca^{2+} sensitization. Error bars indicate S.E.M. *, significantly different (Student's t test, $P < 0.05$).

ERK and p38MAPK Contribute to Elevated CCH-Induced Contraction in Circular Smooth Muscle in DSS Colitis. Because ERK and p38MAPK are known to mediate Ca^{2+} sensitization in smooth muscle (Gerthoffer, 2005; Murthy, 2006; Ihara et al., 2007), we next investigated whether these MAPK pathways contributed to the increase in CCh-induced Ca^{2+} sensitization found in DSS-induced colitis. First, the relative contribution of ERK, p38MAPK, or ROK pathways to CCh-induced contraction was examined in colonic circular smooth muscle of normal mice. Then, the impact of colitis on the relative contribution of the different protein kinases to CCh-induced Ca^{2+} sensitization was ex-

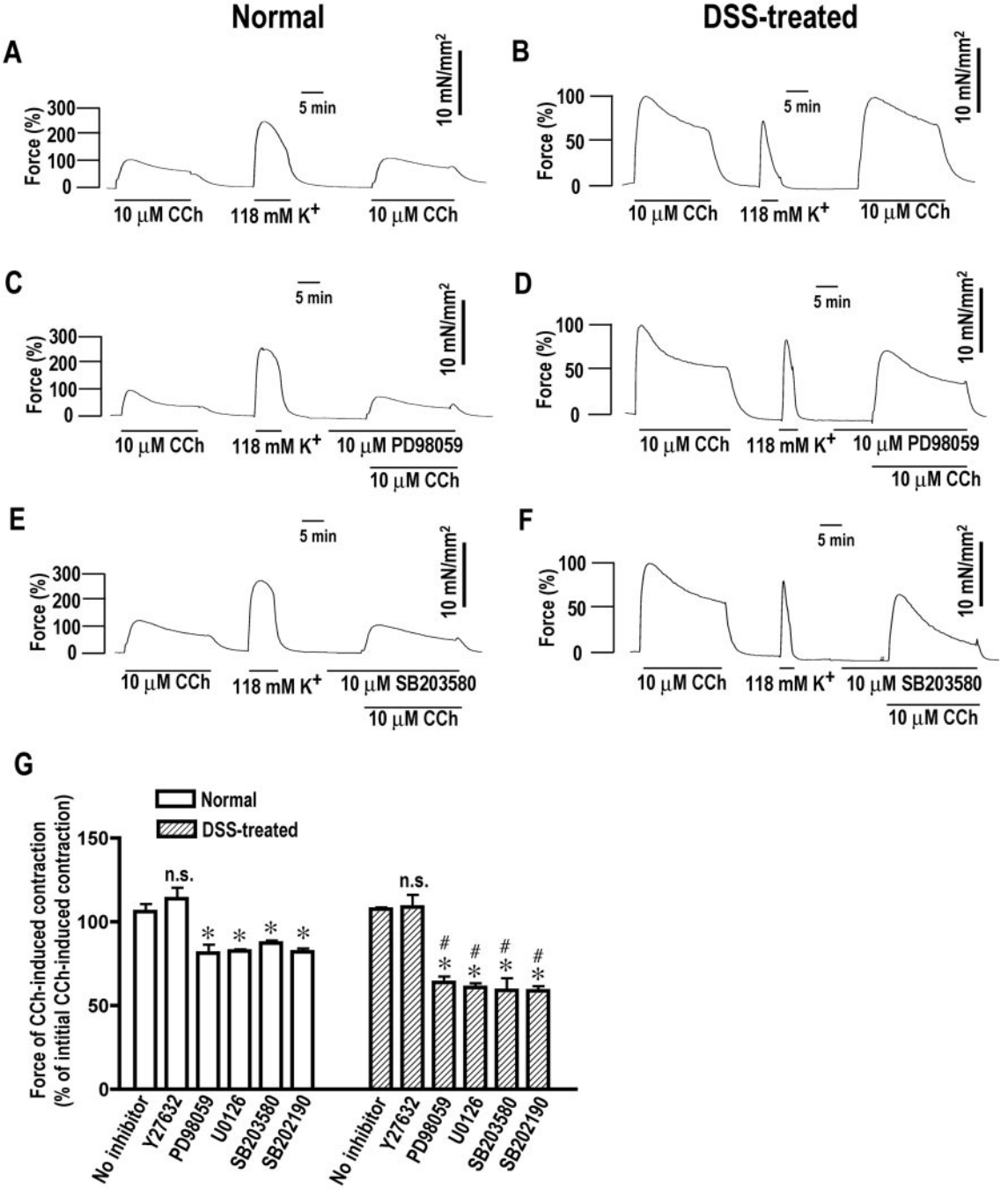

Fig. 4. Effects of MAPK and ROK inhibitors on carbachol (CCh)-induced contraction in colonic circular smooth muscle strips from normal and DSS-treated mice. A to F, representative recordings of CCh-induced contraction in colonic circular smooth muscle strips from normal mice in the absence (A) or presence of pharmacological inhibitors including MEK1/2 (PD98059) (C) and p38MAPK (SB203580) (E), and representative recordings of CCh-induced contraction in colonic circular smooth muscle strips from DSS-treated mice in the absence (B) or presence of PD98059 (D) or SB203580 (F). After CCh was washed out with NES, the strips were stimulated once with 118 mM K^+ before the re-application of CCh (10 μM). Each protein kinase inhibitor was added 10 min before the re-application of CCh. G, the cumulative results are representative of 4 independent experiments for effects of various inhibitors on CCh-induced contraction: Y27632 (ROK, 10 μM), PD98059 (MEK1/2, 10 μM), U0126 (MEK1/2, 10 μM), SB203580 (p38MAPK, 10 μM) and SB202190 (p38MAPK, 10 μM). The maximal force level during the contraction induced by the first application of CCh was designated as 100% in each strip. Error bars indicate S.E.M. *, significantly different from control response (no inhibitor) (Student's t test, $P < 0.05$). #, significantly different from the value obtained in normal mice in the presence of indicated protein kinase inhibitors (Student's t test, $P < 0.05$).

amined. Muscle strips were subjected to sequential treatment with CCh (10 μM) in NES. The response to the first CCh stimulation was used as a reference for the subsequent contraction produced when protein kinase inhibitors were included. Assays to measure ERK and p38MAPK kinase activities in homogenates of smooth muscles after treatment with 10 μM PD98059 and SB203580 indicate that PD98059 and SB203580 applications could reduce ERK and p38MAPK activity by 75.6 ± 5.6 and 54.5 ± 10.4%, respectively (Supplemental Fig. 2). The maximal contractile force obtained with the second CCh stimulation (106.1 ± 4.6, $n = 4$) was not different from that obtained during the first stimulation, assigning the maximal force level induced by the first CCh to be 100% (Fig. 4, A and G). Pharmacological inhibitors of the ROK pathway (Y27632), ERK pathway (MEK1/2, PD98059, and U0126) and p38MAPK pathway (SB203580 and SB202190) were applied 10 min before the second stimulation with CCh. There was a small but significant reduction in the CCh-induced contraction of smooth muscle obtained in the presence of PD98059 and U0126 (ERK pathway inhibitors), 18.7 ± 5.2% ($n = 4$) and 17.4 ± 1.3% ($n = 4$), respectively (Fig. 4, C and G). There was also a significant reduction in the CCh-induced contraction in the presence of SB203580 and SB202190 (p38MAPK pathway inhibitors), 12.6 ± 1.8% ($n = 4$) and 18.0 ± 2.4% ($n = 4$), respectively (Fig. 4, E and G). Y27632 (ROK pathway inhibitor) had no effect on CCh-induced contraction (Fig. 4G).

In DSS-treated mice, the contractile force obtained in the presence of PD98059 or SB203580 was reduced by 63.8 ± 3.7% ($n = 4$) and 49.0 ± 7.2% ($n = 4$), respectively (Fig. 4D). Furthermore, similar results were obtained with U0126 and SB202190. The contributions of ERK and p38MAPK pathways to CCh-induced contraction were significantly increased in inflamed relative to control colonic smooth muscle. Treatment with Y27632 did not affect CCh-induced contraction in DSS-treated mice (Fig. 4G). In summary, MAPKs (including ERK and p38MAPK) but not ROK contributed to CCh-induced contraction in normal colonic circular smooth muscle. Moreover, both ERK and p38MAPK were associated with the potentiation of CCh-induced contraction in acute inflamed colonic circular smooth muscle.

Ca^{2+} Sensitization Can Be Unmasked by Microcystin and Is Increased in DSS Colitis. The application of microcystin (an inhibitor of protein phosphatase 1 and 2A) to smooth muscle can unmask the basal activity of Ca^{2+}-independent protein kinases to generate Ca^{2+}-independent contraction. The force generated by microcystin is attributed to Ca^{2+}-sensitizing protein kinase pathways and is also associated with diphosphorylation of LC_{20} at Ser-19 and Thr-18 (Ihara and Macdonald, 2007; Ihara et al., 2007). Next, we examined whether Ca^{2+}-independent contraction was altered in DSS colitis. When microcystin was applied to β-escin permeabilized colonic circular smooth muscle strips at pCa 9.0, the force gradually developed and reached a plateau within 45 min (Fig. 5A). It is noteworthy that this contraction was potentiated in the DSS-treated mice (Fig. 5B); both the initial and sustained forces generated were significantly higher than those obtained in normal mice (Fig. 5C). We examined whether the increase in microcystin-induced contraction was associated with increased LC_{20} phosphorylation. The microcystin-induced contraction was accompanied by mono- and diphosphorylation of LC_{20} in normal mice (Fig. 5D), 18.6 ± 1.2% ($n = 4$) and 3.13 ± 0.56% ($n = 4$) of total LC_{20}, respectively. This corresponds to an overall phosphorylation stoichiometry of 0.25 mol of P_i/mol of LC_{20}. In contrast, for DSS-treated mice, the extent of LC_{20} mono- and diphosphorylation during microcystin-induced contraction was 20.9 ± 0.89% ($n = 4$) and 7.4 ± 0.94% ($n = 4$) of total

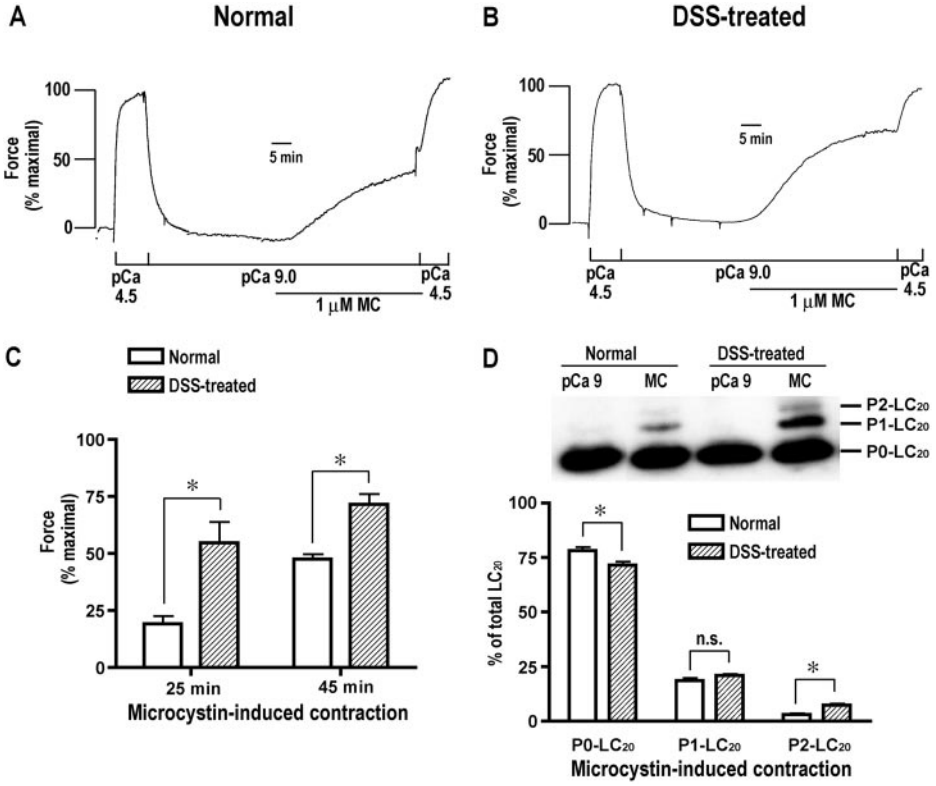

Fig. 5. Microcystin-induced Ca^{2+}-sensitized contraction in β-toxin permeabilized colonic circular smooth muscle strips from normal and DSS-treated mice. A and B, microcystin-induced, Ca^{2+}-sensitized contraction of colonic smooth muscle was measured for normal (A) and DSS-treated mice (B). Microcystin (1 μM) was applied to the strips in pCa 9 solution. Forces observed at pCa 9 and pCa 4.5 were designated as 0% and 100%, respectively. C, the cumulative results are representative of 5 independent experiments for microcystin-induced, Ca^{2+}-sensitized contraction. D, after the treatment of colonic smooth muscle with microcystin (1 μM; 45 min), LC_{20} phosphorylation was measured by Phos-Tag SDS-PAGE. Different exposure times were used for quantification to ensure that signals lay within the linear range of signal intensity. Data are expressed as a % of total LC_{20} for unphosphorylated (P0-LC_{20}), monophosphorylated (P1-LC_{20}) and diphosphorylated (P2-LC_{20}) bands. Error bars indicate S.E.M., $n = 5$ independent experiments. *, significantly different from control (Student's t test, $P < 0.05$); n.s., not significantly different from control.

LC_{20}, respectively (Fig. 5D). The overall phosphorylation stoichiometry (0.36 mol of P_i/mol of LC_{20}) was also significantly higher than that obtained with control mice. These results show that increase in diphosphorylation of LC_{20} is associated with smooth muscle contractile dysfunction with DSS-induced colitis in a manner similar to those observed with vascular diseases such as vasospasm (Katsumata et al., 1997).

ERK and p38MAPK Potentiate Ca^{2+}-Independent Contraction in DSS Colitis. Next, we investigated whether ERK and/or p38MAPK contributed to microcystin-induced Ca^{2+}-independent contraction in colonic circular smooth muscle. Because PD98059 (a MEK1/2 inhibitor) and SB203580 (a p38MAPK inhibitor) work in a manner similar to that of U0126 and SB202190, respectively (Fig. 4G), PD98059 and SB203580 were selected for use in subsequent experiments. We reported previously that the ERK and p38MAPK pathways, but not the ROK pathway, contribute to microcystin-induced contraction in intestinal smooth muscle (Ihara et al., 2007). We were surprised to find that, unlike rat ileal smooth muscle, the MAPK inhibitors were ineffective toward microcystin-induced contraction in normal mice. It is noteworthy that the enhancement of microcystin-induced, Ca^{2+}-independent contraction observed in DSS-treated mice was inhibited with PD98059 and SB203580, but not with Y27632 (Fig. 6). These results suggest that ERK and p38MAPK signaling pathways are upregulated and become the dominant contributors to Ca^{2+}-independent contraction in inflamed colonic circular smooth muscle. Taken together, the ERK and p38MAPK signaling pathways become the dominant contributors to potentiated contractility not only with agonist-induced contraction in the presence of extracellular Ca^{2+} (1.2 mM) in intact colonic circular smooth muscle strips but also with microcystin-induced Ca^{2+}-independent contraction in β-escin permeabilized colonic circular smooth muscle strips.

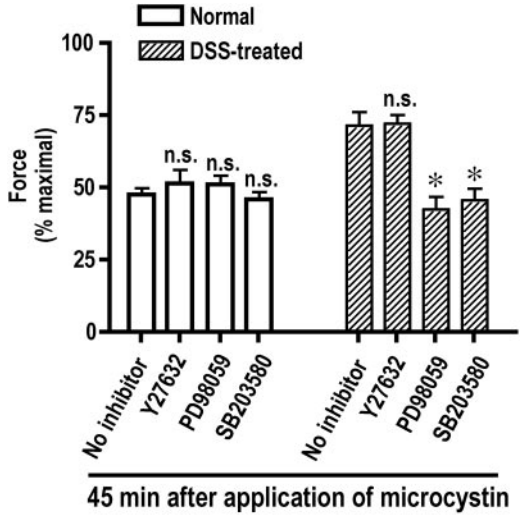

Fig. 6. Effects of MAPK and ROK inhibitors on the potentiation of microcystin-induced Ca^{2+}-sensitized contraction in β-toxin permeabilized colonic circular smooth muscle strips from DSS-treated mice. Pharmacological inhibitors of ROK (Y27632, 10 μM), MEK1/2 (PD98059, 10 μM) and p38 MAPK (SB203580, 10 μM) were applied to colonic smooth muscle of normal and DSS-treated mice. Microcystin (1 μM)-induced contraction was determined 20 min after application of protein kinase inhibitors. Error bars indicate S.E.M., $n = 5$ independent experiments. *, significantly different from control (Student's t test, $P < 0.05$); n.s., not significantly different from control.

ERK and p38MAPK Expressions Are Up-Regulated in Circular Smooth Muscle in Colitis. Because both ERK and p38MAPK pathways were associated with hypercontractility and potentiation of Ca^{2+} sensitization in inflamed colonic circular smooth muscle, we examined whether the expression levels of ERK and/or p38MAPK were also upregulated. Immunohistochemistry revealed that ERK was expressed not only in the submucosa but also in the muscularis propria of colonic sections from normal mice (Fig. 7A). Positive immunostaining for phospho-ERK was also observed in muscularis propria of normal mice. Immunostaining for total-p38MAPK and phospho-p38MAPK was also observed in muscularis propria of normal mice, but staining was diffuse (Fig. 7B). As expected, positive immunostaining both for total-ERK and phospho-ERK were significantly increased in the muscularis propria in the inflamed DSS-treated mice (Fig. 7A). Likewise, positive immunostaining for both total p38MAPK and phospho-p38MAPK were also increased in the muscularis propria after DSS treatment (Fig. 7B). To offer further support of these findings, we also carried out Western blot analyses for total ERK and total p38MAPK from isolated colonic circular smooth muscle. Consistent with the immunohistochemistry results, the expression of ERK and p38MAPK was increased, 3.3- and 2.9-fold, respectively, in colonic smooth muscle from DSS-treated mice (Fig. 7, C and D). Taken together, our results indicate that ERK and p38MAPK pathways in colonic smooth muscle were up-regulated in a T_H2 model of experimental colitis. We next examined whether the expression of ERK and p38MAPK was also altered in human colonic smooth muscle from patients with IBD. Immunohistochemistry of total ERK and total p38MAPK was carried out for human colonic sections from patients without IBD (normal) and with IBD (CD or UC) (Fig. 7E). The positive staining of total ERK in the muscularis propria was increased in sections from patients with IBD compared with non-IBD controls. It is noteworthy that the ERK staining was much greater in UC ($P < 0.0001$) than in CD ($P = 0.012$). Alternatively, p38MAPK was increased in muscularis propria from patients with UC ($P = 0.001$) but not with CD ($P = 0.23$) compared with non-IBD controls. Our results indicate that contractile dysfunction in IBD involves changes in Ca^{2+} sensitization pathways as well as alteration in the MAPK pathways and that the T_H2 environment influences these events.

Discussion

Alterations in Ca^{2+} sensitization have been shown to underlie many diseases associated with smooth muscle dysfunction (Seko et al., 2003; Miwa et al., 2005). Under inflammatory conditions, it is thought that intestinal smooth muscle undergoes a phenotypic change in which normal rhythmic contractions are supplanted by sustained Ca^{2+}-independent contractions that persist long after mucosal healing (Moreels et al., 2001). In the present study, we show that Ca^{2+} sensitization is increased in inflamed colonic circular smooth muscle of BALB/c mice, a T_H2 mouse model of experimental colitis. Furthermore, we demonstrate for the first time that the potentiation of Ca^{2+} sensitization and induction of hypercontractility in colonic muscle during inflammation can be mediated by MAPKs. The Ca^{2+}-calmodulin/MLCK pathway is the primary mediator of contraction after membrane depolarization; however, many signaling pathways, in addi-

tion to the Ca^{2+}-calmodulin/MLCK pathway, are activated via CCh stimulation of muscarinic receptors (Murthy, 2006). The stimulation of M_3 receptors, which are coupled to $G_{q/11}$, activates phospholipase C and produces inositol 1,4,5-trisphosphate and diacylglycerol. These second messengers elicit the activation of protein kinase C and trigger an increase in $[Ca^{2+}]_i$ (Gerthoffer, 2005). Although the inhibition of adenylyl cyclase is a classic and established effect of M_2 receptor activation in smooth muscle, other downstream signaling pathways are believed to be coupled to the M_2 receptors, including Src family tyrosine kinases (Singer et al., 2002) and MAPKs (Cook et al., 2000). We have previously

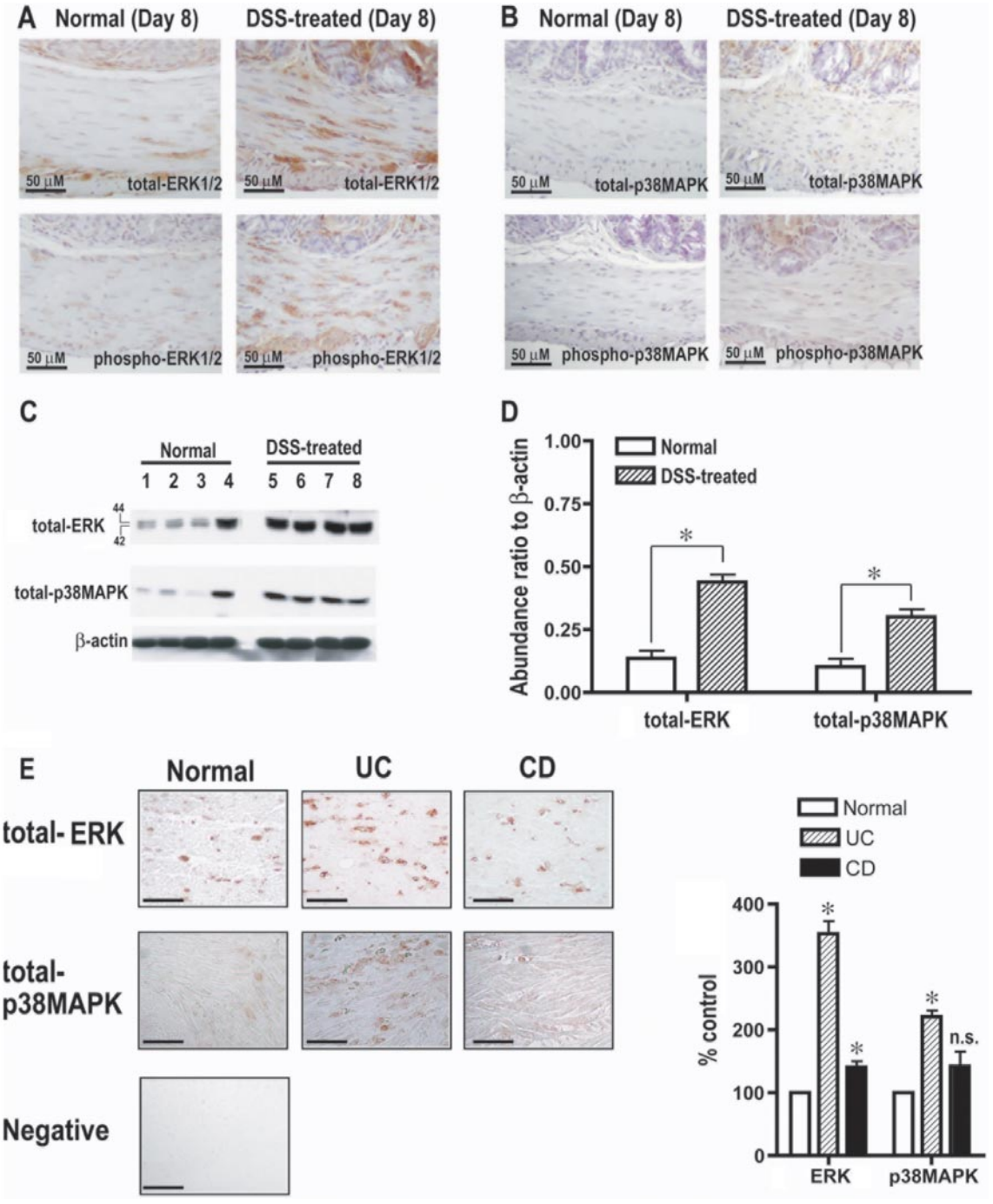

Fig. 7. Expression levels of ERK and p38MAPK in colonic circular smooth muscle of normal and DSS-treated mice, and immunohistochemical detection of ERK in human sections from normal and IBD colon. A and B, deparaffinized colonic tissue sections of normal and DSS-treated mice were probed with (A) ERK and phospho-ERK and (B) p38MAPK and phospho-p38MAPK antibodies. Standard immunohistochemical controls (e.g., no primary antibody) were negative. Bar, 50 μm. C and D, Western blot analysis of total-ERK and total-p38MAPK from isolated colonic circular smooth muscle of normal and DSS-treated mice (C). Each lane shows the protein expression from a single mouse (lanes 1–4, normal mice; lanes 5–8, DSS-treated mice). The cumulative results obtained from 4 independent experiments are shown (D). $*$, significantly different (Student's t test, $P < 0.05$). E, immunohistochemistry results of total-ERK and total-p38MAPK for human colonic sections from patients with non-IBD (normal) and IBD (Crohn's disease or ulcerative colitis). Standard controls (e.g., no primary antibody) were negative. Bar indicates 50 μm. The quantitative comparison of immunostaining for total-ERK and total-p38MAPK obtained with blinded sections from $n = 3$ separate patients. Densitometric analysis of immunostaining was performed with Image J software. Data are expressed as a percentage of immunostaining in normal (non-IBD) smooth muscle.

demonstrated that ERK and p38MAPK are important mediators of Ca^{2+} sensitization in rat ileal smooth muscle (Ihara et al., 2007). None of these protein kinases contributed significantly to Ca^{2+}-independent contraction of colonic circular smooth muscle from normal BALB/c mice; thus, there seems to be less potential for activation of Ca^{2+} sensitization within mouse colonic smooth muscle under normal conditions. Although ERK and p38MAPK played only a minor role in CCh-induced contraction of intact colonic circular smooth muscle from normal BALB/c mice, these kinases were stimulated under inflammatory conditions to play a prominent role in Ca^{2+} sensitization both during CCh-induced contraction of intact colonic circular smooth muscle strips and microcystin-induced contraction of β-escin permeabilized strips. These findings are supported by immunohistochemistry and Western blot results that illustrate increased expression and phosphorylation of ERK and p38MAPK in muscularis propria during acute inflammation. Furthermore, we have shown that ERK and p38MAPK expressions were enhanced in human colonic smooth muscle of patients with UC, also thought to exhibit a T_H2-like cytokine profile (Heller et al., 2005).

In our studies, a hyper-responsiveness of colonic smooth muscle to CCh-induced Ca^{2+} sensitization was associated with acute inflammation and a predominant T_H2 cytokine response. BALB/c mice have an increased propensity to respond to various inflammatory stimulators in a T_H2 fashion (Karupiah, 1998). Although few generalizations can be made, it seems that contractile dysfunction depends on the specific inflammatory environment. Decreased smooth muscle contractility has been observed with other models of intestinal inflammation. The induction of TNF-α and colonic inflammation by TNBS in C57BL/6 mice (Kinoshita et al., 2006b; Ohama et al., 2007), attenuated CCh-induced contraction. In this colitis model, decreased activities of CPI-17 (Ohama et al., 2007) and L-type Ca^{2+} channels (Kinoshita et al., 2003) played central roles in the suppression of CCh-induced contractile responses. Other reports suggest that T_H2 cytokines are consistently associated with smooth muscle hypercontractility. Infection of C57BL/6 mice with *Trichinella spiralis* results in a T_H2 response and jejunal smooth muscle hypercontractility (Akiho et al., 2002, 2005a). Alternatively, adenovirus-mediated IL-4 gene transfer to the jejunal serosa leads to jejunal longitudinal smooth muscle hyperresponsiveness to CCh in C57BL/6 mice (Vallance et al., 2007). Although the precise mechanisms whereby T_H2 cytokines mediate hypercontractility were not identified, both IL-4 and IL-13 could contribute to nematode-associated intestinal smooth muscle hypercontractility via STAT6 (Akiho et al., 2002, 2005b). Our results suggest that T_H2 cytokines contribute to smooth muscle Ca^{2+} sensitization and hypercontractility via activation of ERK and p38MAPK; because increases in IL-13 were not observed in our model of colitis, an IL-4/STAT6 mechanism could be a candidate for activation of these protein kinases.

The precise mechanisms by which MAPKs regulate smooth muscle contraction are not fully understood. In one scenario, MAPK activation can increase the Mg^{2+}-ATPase activity of myosin II. ERK has been shown to phosphorylate caldesmon, a thin-filament associated protein that prevents the binding of myosin to actin (Sobue and Sellers, 1991). The phosphorylation of caldesmon by ERK weakens the affinity of caldesmon toward actin (Huang et al., 2003) and hence promotes cross-bridge cycling and force development. Alternatively, p38MAPK has been shown to phosphorylate and activate MAPK-activated protein kinase 2 (Cohen, 1997), which in turn can phosphorylate the 27-kDa heat shock protein (HSP27) (Rouse et al., 1994). Phosphorylated HSP27 was able to reverse the inhibitory effects of caldesmon on Mg^{2+}-ATPase activity of myosin II (Sobue and Sellers, 1991; Somara and Bitar, 2006). Alternatively, MAPKs contribute to smooth muscle contraction through the regulation of MLCP activity. The ERK pathway was reported to regulate Ca^{2+}-sensitivity and contractility of sheep uterine artery (Xiao et al., 2005), in this case, activation of ERK resulted in increased phosphorylation of myosin target subunit of MLCP (MYPT1) at Thr-853 and inhibition of MLCP activity. Our laboratory has also demonstrated that ERK and p38MAPK pathways contribute to the inhibition of MLCP through changes in the phosphorylation of MYPT1 at Thr-696 (Ihara et al., 2007). There is now a single report that suggests proline-directed kinases such as ERK or p38MAPK can directly phosphorylate MYPT1 (Yamashiro et al., 2008); thus, further investigations will be required to identify the link between MAPK activation and MYPT1 phosphorylation.

The molecular events underlying the phenotypic responses of the intestine to pathological inflammation are reflected in diverse tissue types, including smooth muscle. We have identified the ability of Ca^{2+}-independent signaling pathways to influence contractile properties of intestinal smooth muscle under inflammatory conditions. The p38MAPK and ERK protein kinase pathways are contributors to intestinal hypercontractility under T_H2 mediated inflammatory events. Our studies provide the identification of new therapeutic targets that may aid in the management of patients with IBD-associated smooth muscle dysfunction.

References

Akiho H, Blennerhassett P, Deng Y, and Collins SM (2002) Role of IL-4, IL-13, and STAT6 in inflammation-induced hypercontractility of murine smooth muscle cells. *Am J Physiol Gastrointest Liver Physiol* **282:**G226–G232.

Akiho H, Deng Y, Blennerhassett P, Kanbayashi H, and Collins SM (2005a) Mechanisms underlying the maintenance of muscle hypercontractility in a model of postinfective gut dysfunction. *Gastroenterology* **129:**131–141.

Akiho H, Lovato P, Deng Y, Ceponis PJ, Blennerhassett P, and Collins SM (2005b) Interleukin-4- and -13-induced hypercontractility of human intestinal muscle cells-implication for motility changes in Crohn's disease. *Am J Physiol Gastrointest Liver Physiol* **288:**G609–G615.

Beck PL, Xavier R, Wong J, Ezedi I, Mashimo H, Mizoguchi A, Mizoguchi E, Bhan AK, and Podolsky DK (2004) Paradoxical roles of different nitric oxide synthase isoforms in colonic injury. *Am J Physiol Gastrointest Liver Physiol* **286:**G137–G147.

Borman MA, MacDonald JA, Murányi A, Hartshorne DJ, and Haystead TA (2002) Smooth muscle myosin phosphatase-associated kinase induces Ca^{2+} sensitization via myosin phosphatase inhibition. *J Biol Chem* **277:**23441–23446.

Cohen P (1997) The search for physiological substrates of MAP and SAP kinases in mammalian cells. *Trends Cell Biol* **7:**353–361.

Cook AK, Carty M, Singer CA, Yamboliev IA, and Gerthoffer WT (2000) Coupling of M_2 muscarinic receptors to ERK MAP kinases and caldesmon phosphorylation in colonic smooth muscle. *Am J Physiol Gastrointest Liver Physiol* **278:**G429–G437.

Deng JT, Sutherland C, Brautigan DL, Eto M, and Walsh MP (2002) Phosphorylation of the myosin phosphatase inhibitors, CPI-17 and PHI-1, by integrin-linked kinase. *Biochem J* **367:**517–524.

Eto M, Senba S, Morita F, and Yazawa M (1997) Molecular cloning of a novel phosphorylation-dependent inhibitory protein of protein phosphatase-1 (CPI17) in smooth muscle: its specific localization in smooth muscle. *FEBS Lett* **410:**356–360.

Gerthoffer WT (2005) Signal-transduction pathways that regulate visceral smooth muscle function. III. Coupling of muscarinic receptors to signaling kinases and effector proteins in gastrointestinal smooth muscles. *Am J Physiol Gastrointest Liver Physiol* **288:**G849–G853.

Heller F, Florian P, Bojarski C, Richter J, Christ M, Hillenbrand B, Mankertz J, Gitter AH, Bürgel N, Fromm M, et al. (2005) Interleukin-13 is the key effector T_H2 cytokine in ulcerative colitis that affects epithelial tight junctions, apoptosis, and cell restitution. *Gastroenterology* **129:**550–564.

Huang R, Li L, Guo H, and Wang CL (2003) Caldesmon binding to actin is regulated

by calmodulin and phosphorylation via different mechanisms. *Biochemistry* **42:** 2513–2523.
Ihara E and MacDonald JA (2007) The regulation of smooth muscle contractility by zipper-interacting protein kinase. *Can J Physiol Pharmacol* **85:**79–87.
Ihara E, Moffat L, Ostrander J, Walsh MP, and MacDonald JA (2007) Characterization of protein kinase pathways responsible for Ca^{2+} sensitization in rat ileal longitudinal smooth muscle. *Am J Physiol Gastrointest Liver Physiol* **293:**G699–G710.
Karupiah G (1998) Type 1 and type 2 cytokines in antiviral defense. *Vet Immunol Immunopathol* **63:**105–109.
Katsumata N, Shimokawa H, Seto M, Kozai T, Yamawaki T, Kuwata K, Egashira K, Ikegaki I, Asano T, Sasaki Y, et al. (1997) Enhanced myosin light chain phosphorylations as a central mechanism for coronary artery spasm in a swine model with interleukin-1beta. *Circulation* **96:**4357–4363.
Kimura K, Ito M, Amano M, Chihara K, Fukata Y, Nakafuku M, Yamamori B, Feng J, Nakano T, Okawa K, et al. (1996) Regulation of myosin phosphatase by Rho and Rho-associated kinase (Rho-kinase). *Science* **273:**245–248.
Kinoshita E, Kinoshita-Kikuta E, Takiyama K, and Koike T (2006a) Phosphate-binding tag, a new tool to visualize phosphorylated proteins. *Mol Cell Proteomics* **5:**749–757.
Kinoshita K, Hori M, Fujisawa M, Sato K, Ohama T, Momotani E, and Ozaki H (2006b) Role of TNF-α in muscularis inflammation and motility disorder in a TNBS-induced colitis model: clues from TNF-α-deficient mice. *Neurogastroenterol Motil* **18:**578–588.
Kinoshita K, Sato K, Hori M, Ozaki H, and Karaki H (2003) Decrease in activity of smooth muscle L-type Ca^{2+} channels and its reversal by NF-κB inhibitors in Crohn's colitis model. *Am J Physiol Gastrointest Liver Physiol* **285:**G483–G493.
Kiss E, Murányi A, Csortos C, Gergely P, Ito M, Hartshorne DJ, and Erdodi F (2002) Integrin-linked kinase phosphorylates the myosin phosphatase target subunit at the inhibitory site in platelet cytoskeleton. *Biochem J* **365:**79–87.
MacDonald JA, Eto M, Borman MA, Brautigan DL, and Haystead TA (2001) Dual Ser and Thr phosphorylation of CPI-17, an inhibitor of myosin phosphatase, by MYPT-associated kinase. *FEBS Lett* **493:**91–94.
Miwa K, Fujita M, and Sasayama S (2005) Recent insights into the mechanisms, predisposing factors, and racial differences of coronary vasospasm. *Heart Vessels* **20:**1–7.
Moreels TG, De Man JG, Dick JM, Nieuwendijk RJ, De Winter BY, Lefebvre RA, Herman AG, and Pelckmans PA (2001) Effect of TNBS-induced morphological changes on pharmacological contractility of the rat ileum. *Eur J Pharmacol* **423:** 211–222.
Murthy KS (2006) Signaling for contraction and relaxation in smooth muscle of the gut. *Annu Rev Physiol* **68:**345–374.
Neurath MF, Finotto S, and Glimcher LH (2002) The role of Th1/Th2 polarization in mucosal immunity. *Nat Med* **8:**567–573.
Ohama T, Hori M, Momotani E, Iwakura Y, Guo F, Kishi H, Kobayashi S, and Ozaki H (2007) Intestinal inflammation downregulates smooth muscle CPI-17 through induction of TNF-alpha and causes motility disorders. *Am J Physiol Gastrointest Liver Physiol* **292:**G1429–G1438.
Rouse J, Cohen P, Trigon S, Morange M, Alonso-Llamazares A, Zamanillo D, Hunt T, and Nebreda AR (1994) A novel kinase cascade triggered by stress and heat shock that stimulates MAPKAP kinase-2 and phosphorylation of the small heat shock proteins. *Cell* **78:**1027–1037.
Seko T, Ito M, Kureishi Y, Okamoto R, Moriki N, Onishi K, Isaka N, Hartshorne DJ, and Nakano T (2003) Activation of RhoA and inhibition of myosin phosphatase as important components in hypertension in vascular smooth muscle. *Circ Res* **92:** 411–418.
Singer CA, Vang S, and Gerthoffer WT (2002) Coupling of M_2 muscarinic receptors to Src activation in cultured canine colonic smooth muscle cells. *Am J Physiol Gastrointest Liver Physiol* **282:**G61–G68.
Sobue K and Sellers JR (1991) Caldesmon, a novel regulatory protein in smooth muscle and nonmuscle actomyosin systems. *J Biol Chem* **266:**12115–12118.
Somara S and Bitar KN (2006) Phosphorylated HSP27 modulates the association of phosphorylated caldesmon with tropomyosin in colonic smooth muscle. *Am J Physiol Gastrointest Liver Physiol* **291:**G630–G639.
Somlyo AP and Somlyo AV (1994) Signal transduction and regulation in smooth muscle. *Nature* **372:**231–236.
Somlyo AP and Somlyo AV (2003) Ca^{2+} sensitivity of smooth muscle and nonmuscle myosin II: modulated by G proteins, kinases, and myosin phosphatase. *Physiol Rev* **83:**1325–1358.
Takeya K, Loutzenhiser K, Shiraishi M, Loutzenhiser R, and Walsh MP (2008) A highly sensitive technique to measure myosin regulatory light chain phosphorylation: the first quantification in renal arterioles. *Am J Physiol Renal Physiol* **294:**F1487–F1492.
Vallance BA, Radojevic N, Hogaboam CM, Deng Y, Gauldie J, and Collins SM (2007) IL-4 gene transfer to the small bowel serosa leads to intestinal inflammation and smooth muscle hyperresponsiveness. *Am J Physiol Gastrointest Liver Physiol* **292:**G385–G394.
Xavier RJ and Podolsky DK (2007) Unravelling the pathogenesis of inflammatory bowel disease. *Nature* **448:**427–434.
Xiao D, Longo LD, and Zhang L (2005) α_1-adrenoceptor-mediated phosphorylation of MYPT-1 and CPI-17 in the uterine artery: role of ERK/PKC. *Am J Physiol Heart Circ Physiol* **288:**H2828–H2835.
Yamashiro S, Yamakita Y, Totsukawa G, Goto H, Kaibuchi K, Ito M, Hartshorne DJ, and Matsumura F (2008) Myosin phosphatase-targeting subunit 1 regulates mitosis by antagonizing polo-like kinase 1. *Dev Cell* **14:**787–797.

Address correspondence to: Justin A. MacDonald, Smooth Muscle Research Group, Department of Biochemistry and Molecular Biology, University of Calgary, Faculty of Medicine, 3330 Hospital Drive N.W., Calgary, Alberta, T2N 4N1, Canada. E-mail: jmacdo@ucalgary.ca